



**HAL**  
open science

## Preparation and characterisation of $\text{Pu}_{0.5}\text{Am}_{0.5}\text{O}_2 - x\text{-MgO}$ Ceramic/Ceramic composites

A. Jankowiak, F. Jorion, C. Maillard, L. Donnet

► **To cite this version:**

A. Jankowiak, F. Jorion, C. Maillard, L. Donnet. Preparation and characterisation of  $\text{Pu}_{0.5}\text{Am}_{0.5}\text{O}_2 - x\text{-MgO}$  Ceramic/Ceramic composites. Nuclear Science and Engineering, 2017, 160 (3), pp.378-384. 10.13182/NSE160-378 . cea-02512131

**HAL Id: cea-02512131**

**<https://cea.hal.science/cea-02512131>**

Submitted on 19 Mar 2020

**HAL** is a multi-disciplinary open access archive for the deposit and dissemination of scientific research documents, whether they are published or not. The documents may come from teaching and research institutions in France or abroad, or from public or private research centers.

L'archive ouverte pluridisciplinaire **HAL**, est destinée au dépôt et à la diffusion de documents scientifiques de niveau recherche, publiés ou non, émanant des établissements d'enseignement et de recherche français ou étrangers, des laboratoires publics ou privés.

# Fabrication and characterisation of $\text{Pu}_{0.5}\text{Am}_{0.5}\text{O}_{2-x}$ -MgO Cercer composites

A. Jankowiak<sup>a\*</sup>, F. Jorion<sup>a</sup>, C. Maillard<sup>b</sup>, L. Donnet<sup>a</sup>

Commissariat à l'Energie Atomique (CEA)

<sup>a</sup> CEA/DEN/VRH/DTEC/STCF/LEMA

<sup>b</sup> CEA/DEN/VRH/DRCP/SE2A/LEHA

30207 Bagnols-sur-Cèze cedex

France

\*corresponding author

tel : +33 4 66 79 65 42

fax: +33 4 66 79 16 49

email : aurelien.jankowiak@cea.fr

## Abstract

This study describes the fabrication and characterisation of  $\text{Pu}_{0.5}\text{Am}_{0.5}\text{O}_{2-x}$ -MgO Cercer composites with 20 and 30vol% of  $\text{Pu}_{0.5}\text{Am}_{0.5}\text{O}_{2-x}$ . The  $\text{Pu}_{0.5}\text{Am}_{0.5}\text{O}_{2-x}$  content was found to result in a change in the reduction behaviour in the composites when exposed to a reducing sintering cycle. This phenomenon could be explained by the percolation theory when applied to the oxygen diffusivity in a randomly distributed binary system. The composites were studied by combined XRD and O/M ratio measurements. Both composites exhibit various amount of bcc and fcc phases which correspond to different reduction states in the mixed actinides compound. It was found that a critical volume fraction of  $\text{Pu}_{0.5}\text{Am}_{0.5}\text{O}_{2-x}$  in the composite exists resulting in an increase of the reduction of this latter compound.

**KEYWORDS:** fuel, americium, plutonium, Cercer, transmutation, reduction

## 1. Introduction

Transmutation of highly active long-lived nuclides into shorter life nuclides is one of the most promising options to reduce wastes radiotoxicity and to provide better storage safety. Due to their peculiar in pile neutronic behaviour, transmutation of minor actinides requires specific fuel cycle combined with dedicated reactor concepts such as Fast Neutrons Reactors (FNR) or

Accelerator Driven Systems (ADS). The potentiality of this option in combination with waste management is widely investigated in numerous countries. FUTURIX-FTA project (FUels for Transmutation of transURanium elements in phenIX / Fortes Teneurs en Actinides [high actinide content]) is an international irradiation program that aims to demonstrate the feasibility of transmuting minor actinides in fast neutron reactors mainly from the standpoint of fuel fabrication and behaviour. It is being pursued jointly by the US Department of Energy (DOE), the Japan Atomic Energy Research Institute (JAERI), the Institute for Transuranium Elements (ITU) in Germany and the Commissariat à l’Energie Atomique in France. The various materials developed for this program are reported in table 1. The irradiation experiment should begin in the PHENIX reactor in 2007 for 240 EFPD [1-2]. In this study, the materials being studied are dense  $(\text{Pu}_{0.5}\text{Am}_{0.5})\text{O}_{2-x}\text{-MgO}$  composites developed in the CEA. Our approach was to investigate the determining role of the mixed actinides oxides content on the reduction behaviour of the composites. Two different compositions were prepared and studied by XRD and thermogravimetric analysis. The first composition PA20 contained 20vol% of  $(\text{Pu}_{0.5}\text{Am}_{0.5})\text{O}_{2-x}$  which was assumed to be the critical volume fraction of this compound in the composite. The second composition PA30 contained 30vol% of  $(\text{Pu}_{0.5}\text{Am}_{0.5})\text{O}_{2-x}$  which was assumed to be beyond the critical volume fraction. Both composites were subjected to a reducing sintering cycle leading to various O/M ratios in the mixed actinides compound.

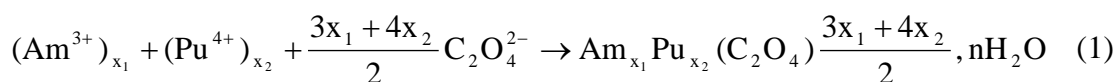
## 2. Experimental procedure

### 2.1. Materials

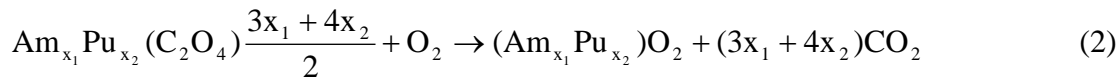
#### 2.1.1. $\text{Pu}_{0.5}\text{Am}_{0.5}\text{O}_2$ synthesis

$(\text{Pu}_{0.5}\text{Am}_{0.5})\text{O}_2$  powder was obtained by oxalate co-conversion technique. It was used as an alternative to solid state reaction in order to reduce the chemical pollution and to limit the risk of contamination by dispersion of solid matter. This technique includes two steps:

- Formation of a precipitate in nitric acid medium with an excess of oxalate



- Calcinations under air to obtain the mixed oxide



The key parameters ( $[\text{HNO}_3]$ ,  $[\text{H}_2\text{C}_2\text{O}_4]_{\text{excess}}$ ) were carefully selected on the basis of the Am and Pu oxalate solubility curves versus  $[\text{HNO}_3]$  and  $[\text{H}_2\text{C}_2\text{O}_4]$  according to [3-8]. Synthesizing mixed  $(\text{Pu}_{1-x}\text{Am}_x)\text{O}_2$  compounds by oxalate co-conversion yields pure single-phase precursors. A uniform black powder was obtained after synthesis and milling. Chemical analysis was performed on the starting solutions, the elemental composition of precursor was found to be in good agreement with the chosen cations atomic ratio (e.g.: 50/50).

### 2.1.2. Magnesium oxide

Magnesia was chosen as an inert matrix due to its high stability both at high temperature and under irradiation [4]. Commercially available magnesia (CERAC 99.95%) was used and firstly calcined at 800°C for 4h to remove moisture. The powder was stored under controlled atmosphere.

## 2.2 Ceric fabrication

The  $(\text{Pu}_{0.5}\text{Am}_{0.5})\text{O}_2$  and MgO powders were weighed and mixed to adjust the final compositions. The mixed Pu/Am oxide and magnesia powders were blended in a ball-type mill during 30min at 30Hz. The mixtures were granulated at 150 $\mu\text{m}$  and pellets were shaped by uniaxial pressing at 400MPa with stearic acid addition. The thermal cycle was carried out under Ar/H<sub>2</sub> 4% up to 1000°C and under pure Ar up to the holding temperature which was set at 1600°C for 4 hours. Figure 1 summarizes the process.

## 3. Results

The sintered pellets were firstly submitted to a visual inspection. Neither crack nor strain was detected. The densities of the sintered samples are reported in Table 2 where it can be seen that PA20 sample exhibits a higher density than that of the PA30 sample.

### 3.1. Microstructural characteristics

Microstructure observations were performed on finely polished axial and radial cross sections on different samples using Jeol SEM. Typical microstructures of  $\text{Pu}_{0.5}\text{Am}_{0.5}\text{O}_{2-x}$

MgO are presented in figure 2. The mixed actinides compound appears in light grey and the magnesia matrix in dark grey. The microstructure exhibits a good homogeneity with a low amount of porosity.

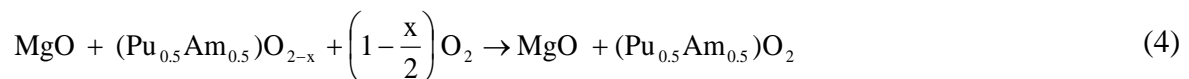
The actinide particle distribution (HD) has been determined by image analysis [5] with an optical microscope POLARON (magnificence X10) on the samples cross sections divided in 20 identical fields. Each field was analysed to evaluate the percentage of surface occupied by the actinide particles. The HD within the samples has been calculated using equation (3).

$$HD = \frac{\sigma}{M} 100 \quad (3)$$

where M is the average value and  $\sigma$  the standard deviation of Pu/Am oxide particles % (in area) for the whole cross sections. A low HD value indicates a higher level of microstructural homogeneity, with HD=0 corresponding to the ideal case, while  $HD \geq 20$  clearly indicates an inhomogeneous distribution [6]. In this study, both composites exhibit HD values lower than 13, which means an acceptable distribution of the actinides mixed oxide particles within the matrix.

### 3.2. Stoichiometry

Oxygen stoichiometry of the fabricated compound is a key property to study the fuel behaviour in the reactor. It is well known that a reduced oxygen potential limits cladding corrosion that could result in failure under irradiation. This is often the case in oxides containing Am due to the extremely high oxygen potential of  $AmO_{2-x}$  [7-13]. In the study of the solid solution of  $PuO_{2-x}$  and  $AmO_{2-x}$ , an increase in Am content induced a greater sensitivity of the compound to reduction due to the instability of tetravalent Am [8-9]. In this study, the O/M ratio of each sample was obtained by thermogravimetric analysis using an oxidizing atmosphere up to 1250°C. Under such conditions, reaction (4) occurs:



As a consequence, O/M ratios were calculated using equation (5):

$$\frac{O}{M} = 2 \frac{\Delta m \times M_{Pu_{0.5}Am_{0.5}O_2}}{16 \times m_f \times a} \quad (5)$$

where  $\Delta m$  is the weight gain during the cycle,

$M_{\text{Pu}_{0.5}\text{Am}_{0.5}\text{O}_2}$ , the molecular mass of the oxidized actinides compound

$a$ , the weight fraction of the oxidized actinides compound in the Cercer,

$m_f$ , the sample weight after reoxidation.

The O/M ratio of PA30 sample was found to be 1.83 while for PA20 it was estimated to 1.88. In both cases, the reoxidation process is completed under 800°C. These O/M ratios obtained by TGA are mean values of the different  $(\text{Pu}_{0.5}\text{Am}_{0.5})\text{O}_{2-x}$  phases in the composites.

### 3.3. Structural analysis

Crystal structures in  $(\text{Pu}_{0.5}\text{Am}_{0.5})\text{O}_{2-x}\text{-MgO}$  were determined by X-ray diffraction with Bruker D8-Advance diffractometer using Mo anti-cathode. Diffraction line intensity and positions were computed using the profile-fitting programs EVA and TOPAS for the lattice parameter refinement. In order to perform accurate lattice parameter measurements, a gold standard powder was added to the samples. Diffraction patterns of sintered samples were carefully examined to evaluate the reactivity between the  $(\text{Pu}_{1-x}\text{Am}_x)\text{O}_{2-x}$  phases and magnesia. Figure 3 and 4 represent the XRD patterns of the composite crushed samples. No Mg-based compound peaks derived from a reaction phase between the two components was observed. Furthermore, both composites submitted to the TGA oxidizing cycle only exhibited  $(\text{Pu}_{0.5}\text{Am}_{0.5})\text{O}_2$  and MgO phases. This result suggests MgO is mostly inert towards the  $(\text{Pu}_{0.5}\text{Am}_{0.5})\text{O}_{2-x}$  phase. Assuming the fact that Pu/Am ratio (e.g. 50/50) remains constant, we extended the correlation between O/M ratio and the lattice parameter for pure Pu and Am oxides to the mixed  $(\text{Pu}_{0.5}\text{Am}_{0.5})\text{O}_{2-x}$  compound [10]. The extrapolated correlation lines can be used to estimate the O/M ratio of each  $(\text{Pu}_{0.5}\text{Am}_{0.5})\text{O}_{2-x}$  phase as represented in figure 5 [9-11].

In the case of the PA30 composite, the XRD pattern reveals three phases:

(a) magnesia fcc “periclase” phase ( $a=4.211 \text{ \AA}$ );

(b) fcc phase ( $a= 5.408 \text{ \AA}$  and  $\text{O/M}=1.93$ );

(c) bcc phase ( $a/2= 5.480 \text{ \AA}$  and  $\text{O/M}=1.66$ ).

For the PA20 composite, in addition to the magnesia, two phases were found:

(d) fcc phase (  $a= 5.421 \text{ \AA}$  and  $O/M= 1.88$ );

(e) bcc phase (  $a/2= 5.456 \text{ \AA}$  and  $O/M=1.74$ ).

The fcc phases correspond to a near stoichiometry phase while the bcc phases are attributed to most reduced phases and show a greater similarity with  $\text{Am}_2\text{O}_3$  bcc phase ( $a/2=5.51 \text{ \AA}$ )[12] rather than  $\text{Pu}_2\text{O}_3$  ( $a/2=5.525 \text{ \AA}$ )[13] for which the diffraction lines positions and intensities are different. To determine the proportion of each phase in the composites, O/M ratio values obtained from the correlation lines were combined to the O/M mean values determined during the thermogravimetric analysis.

Thus, it is possible to write the following equations systems:

$$x_1P_1 + x_2P_2 = O/M_{\text{Global}} \quad (6)$$

$$P_1 + P_2 = 1 \quad (7)$$

where:

$P_1$  and  $P_2$  represents the molar proportions of each phase and can be considered as weight proportions since the molar masses of the two compounds only differ by 2%;

$x_1$  the O/M of the first phase;

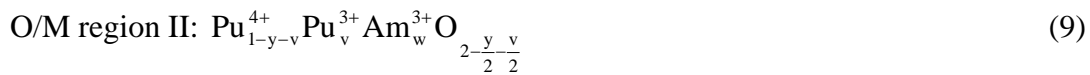
$x_2$  the O/M of the second phase.

In addition to the magnesia phase, the PA30 composite contains 37 wt% of  $(\text{Pu}_{0.5}\text{Am}_{0.5})\text{O}_{1.66}$  and 63 wt% of  $(\text{Pu}_{0.5}\text{Am}_{0.5})\text{O}_{1.93}$  while the PA20 composite only contains 4 wt% of  $(\text{Pu}_{0.5}\text{Am}_{0.5})\text{O}_{1.742}$  reduced phase and 96wt% of  $(\text{Pu}_{0.5}\text{Am}_{0.5})\text{O}_{1.88}$ . The results show that in addition to the magnesia phase, the PA30 composite contains a significantly higher amount of reduced phase if compared to the PA20.

## 4. Discussion

### 4.1. Valence change

In both mixed actinide oxides, Pu and Am have two valence states that could be trivalent and tetravalent. Considering the fact that  $\text{AmO}_{2-x}$  has an higher oxygen potential than  $\text{PuO}_{2-x}$ , Osaka and al. [8] suggested that a O/M ratio decrease from stoichiometry results in Am to be firstly reduced from tetravalent to trivalent state in the first O/M region. Then, Pu is reduced [14] in the second O/M region, according to equations (5) and (6),



Assuming the fact that Pu/Am ratio (e.g.: 50/50) remains constant in both phases, the bcc phase O/M ratio is lower than the boundary O/M ratio between the two regions and defined as  $2-y/2=1.75$ . Following [8] assumption, all Am is reduced from the tetravalent to trivalent state and Pu is partially reduced. The fcc phase has an higher O/M ratio than the boundary O/M ratio which means a partial reduction of Am with all the Pu in tetravalent state. The possible formulae for both phases in the compound are reported in table 3. A first reduction of Am is one of the possible reasons that explains the bcc phase to demonstrate a greater similarity with  $\text{Am}_2\text{O}_3$  than  $\text{Pu}_2\text{O}_3$  phase. A Pu reduction prior Am would have led to a greater similarity with  $\text{Pu}_2\text{O}_3$  phase. This result supports the assumption of Osaka and al. regarding Am prior reduction to Pu and suggests that the phase structure is mainly determined by Am-O system and Am valence change. According to this result, figure 6 presents a possible phase repartition in  $(\text{Pu}_{0.5}\text{Am}_{0.5})\text{O}_{2-x}$  for various O/M varying from 2 to 1.5. The phase existence not only depends on microstructure morphology but also on thermal treatment duration under reducing atmosphere. A further TEM study would be helpful to observe the phase appearance taking into account above mentioned parameters.

## 4.2.Reduction behaviour

As it has already been mentioned, a  $\text{Pu}_{0.5}\text{Am}_{0.5}\text{O}_{2-x}$  increase in the composite results in a increase of the reduced phase amount. It appeared to be a threshold value of 20vol% where the reduction of  $\text{Pu}_{0.5}\text{Am}_{0.5}\text{O}_{2-x}$  compound drastically increases. A possible explanation for this phenomenon is based on the percolation theory [15-16]. This theory can be applied for various diffusion or conduction phenomena. In a binary system, percolation theory predicts that:

if  $v < v_c$

$$D_{\text{composite}} \approx D_A \quad (10)$$

if  $v > v_c$

$$D_{\text{composite}} \approx D_B \quad (11)$$

where:

$v$  is the volume fraction of the phase B;

$v_c$  is critical volume fraction of phase B, or percolation threshold;

$D_A$  is the diffusivity of a specie in the phase A with  $D_A \gg D_B$ ;

$D_B$  is the diffusivity of a specie in the phase B;

$D_{\text{composite}}$  is the diffusivity of that specie in the composite.

In this work, although the oxygen diffusivity in  $\text{Pu}_{0.5}\text{Am}_{0.5}\text{O}_{2-x}$  has never been measured, it may be safe to state that the oxygen diffusivity in MgO is much smaller than that in  $\text{Pu}_{0.5}\text{Am}_{0.5}\text{O}_{2-x}$ . So the relationships of oxygen diffusivity in  $\text{Pu}_{0.5}\text{Am}_{0.5}\text{O}_{2-x} / \text{MgO}$  composites would be:

if  $v > v_c$

$$D_{\text{O}^{2-} \rightarrow \text{composite}} \approx D_{\text{O}^{2-} \rightarrow \text{Pu}_{0.5}\text{Am}_{0.5}\text{O}_{2-x}} \quad (12)$$

if  $v < v_c$

$$D_{\text{O}^{2-} \rightarrow \text{composite}} \approx D_{\text{O}^{2-} \rightarrow \text{MgO}} \quad (13)$$

where:

$v$  is the volume fraction of the phase  $\text{Pu}_{0.5}\text{Am}_{0.5}\text{O}_{2-x}$ ;

$v_c$  is critical volume fraction of phase  $\text{Pu}_{0.5}\text{Am}_{0.5}\text{O}_{2-x}$ ;

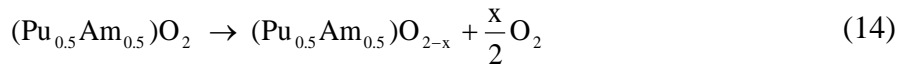
$D_{\text{O}^{2-} \rightarrow \text{Pu}_{0.5}\text{Am}_{0.5}\text{O}_{2-x}}$  is the diffusivity of the oxygen in  $\text{Pu}_{0.5}\text{Am}_{0.5}\text{O}_{2-x}$ ;

$D_{\text{O}^{2-} \rightarrow \text{MgO}}$  is the diffusivity of the oxygen in MgO;

$D_{\text{composite}}$  is the diffusivity of the oxygen in the composite.

From the results, the critical volume fraction  $v_c=20\text{vol}\%$  of  $\text{Pu}_{0.5}\text{Am}_{0.5}\text{O}_{2-x}$  in the composite. This is confirmed by the SEM in figure 2 where PA30 sample microstructure is typical of intermediate to symmetric medium host while PA20 exhibits an asymmetric medium host microstructure [17]. The oxygen diffusivity in a composite with more than 20vol%  $\text{Pu}_{0.5}\text{Am}_{0.5}\text{O}_{2-x}$  should be very close to that in  $\text{Pu}_{0.5}\text{Am}_{0.5}\text{O}_{2-x}$ , which leads to a rapid increase in the formation of a most reduced phase. Similarly, the diffusivity in a composite with  $v < v_c$  should be of the same order as that of MgO (which is very low). Thus,  $\text{Pu}_{0.5}\text{Am}_{0.5}\text{O}_{2-x}$  particles were better protected at high temperature by the matrix and this could explain the lower reduced phase amount.

The outward diffusion of the oxygen from the materials through the surface causes the reduction of  $\text{Pu}_{0.5}\text{Am}_{0.5}\text{O}_{2-x}$  compounds to occur resulting in a weight loss.



For the reduction of  $\text{Pu}_{0.5}\text{Am}_{0.5}\text{O}_{2-x}$  compounds in the composites, a possible oxygen diffusion mechanism is suggested:

If  $v > v_c$

- (i) Oxygen diffusion through the interconnected  $\text{Pu}_{0.5}\text{Am}_{0.5}\text{O}_{2-x}$  phase in white from the core to the surface as shown in figure 7 a.

If  $v < v_c$

- (ii) Oxygen diffusion limited to the  $\text{Pu}_{0.5}\text{Am}_{0.5}\text{O}_{2-x}$  particles located at the surface of the composite as shown in figure 7 b.

This result implies that the reduction phenomenon could be lowered in Ceric composites by limiting the mixed actinides oxide volume under the critical volume fraction and using an inert matrix with a lower sintering temperature and oxygen diffusivity than that of the mixed oxide. Thus, the matrix acts as an oxygen diffusion barrier and protects the fissile particles from excessive reduction. A further study is currently carried out to confirm this result and to establish a complete reduction behaviour percolation curve.

## 5. Conclusion

The fabrication and the characterisation of  $\text{Pu}_{0.5}\text{Am}_{0.5}\text{O}_{2-x}\text{-MgO}$  composites have been described. The effect of  $\text{Pu}_{0.5}\text{Am}_{0.5}\text{O}_{2-x}$  content on the reduction behaviour of the composites developed for the FUTURIX-FTA irradiation experiment was also studied. The reduction behaviour was studied by combined XRD and O/M ratio measurements. Both composites exhibit various amount of bcc and fcc structures which correspond to various reduction state in the mixed actinides compound. From a structural point of view, the XRD datas suggest a reduction of Am prior Pu as possible reason to explain the bcc phase to demonstrate a greater similarity with  $\text{Am}_2\text{O}_3$  than  $\text{Pu}_2\text{O}_3$  phase. In addition to the valence change, the percolation theory applied to the oxygen diffusivity in a randomly distributed binary system could explain the reduction behaviour of the composite. A critical volume fraction of  $\text{Pu}_{0.5}\text{Am}_{0.5}\text{O}_{2-x}$  in the composite was found resulting in an increase of reduction rate of this latter compound when exposed to a reducing thermal cycle. According to this result, the reduction phenomenon of mixed actinides oxide can be reduced in this type of composite by limiting the fissile particles volume under the critical volume fraction and using an inert matrix with a lower oxygen diffusivity than that of the mixed oxide.

## Acknowledgments

The work is performed with support of CEA, DOE, EC and JAERI under the FUTURIX Contract and through the 6<sup>th</sup> Framework programme.

## Captions:

Figure 1: Process of fabrication of  $(\text{Pu}_{0.5}\text{Am}_{0.5})\text{O}_{2-x}\text{-MgO}$  Cerceer

Figure 2: SEM micrograph of a  $\text{Pu}_{0.5}\text{Am}_{0.5}\text{O}_{2-x}\text{-MgO}$  (a) FA30 sample and (b)FA20 sample

Figure 3: XRD patterns of sintered  $(\text{Pu}_{0.5}\text{Am}_{0.5})\text{O}_{2-x}\text{-MgO}$  crushed samples (----) PA30; (—) PA20

Figure 4: XRD patterns of sintered  $(\text{Pu}_{0.5}\text{Am}_{0.5})\text{O}_{2-x}\text{-MgO}$  crushed samples (----) PA30; (—)PA20 showing bcc phase peak

Figure 5: Correlation lines between O/M ratio and the lattice parameter (---)  $\text{PuO}_2$ , (—) $\text{AmO}_2$ , (- →)  $\text{Pu}_{0.5}\text{Am}_{0.5}\text{O}_{2-x}$

Figure 6: Phase repartition in  $(\text{Pu}_{0.5}\text{Am}_{0.5})\text{O}_{2-x}$  for O/M ratio varying from 2 to 1.5

Figure 7: Schematic oxygen diffusion (→) in  $(\text{Pu}_{0.5}\text{Am}_{0.5})\text{O}_{2-x}\text{-MgO}$  (a) FA30 sample (b) FA20 sample (mixed actinides oxide in white, magnesia in dark grey)

Table 1: FUTURIX experimental fuels

Table 2: Cerceer characteristics

Table 3: Possible formula for both phases in the compound

**Tables:**

Pins	Type	Compositions
DOE 1	Metal	35U-29Pu-4Am-2Np30Zr (% wt)
DOE 2	Metal w/o U	48Pu-12Am-40Zr (% wt)
DOE 3	Nitride	(U <sub>0.50</sub> Pu <sub>0.25</sub> Am <sub>0.15</sub> Np <sub>0.10</sub> )N
DOE 4	Nitride w/o U	(Pu <sub>0.50</sub> Am <sub>0.50</sub> )N + 36ZrN (% wt)
ITU 5	Cermet w/o U	(Pu <sub>0.23</sub> Am <sub>0.25</sub> Zr <sub>0.52</sub> )O <sub>2-x</sub> +60vol% Mo
ITU 6	Cermet w/o U	(Pu <sub>0.8</sub> Am <sub>0.2</sub> )O <sub>2-x</sub> +86vol% Mo
CEA 7	Cermet w/o U	(Pu <sub>0.5</sub> Am <sub>0.5</sub> )O <sub>2-x</sub> + 70-80 % vol MgO
CEA 8	Cermet w/o U	(Pu <sub>0.2</sub> Am <sub>0.8</sub> )O <sub>2-x</sub> + 75 % vol MgO

Table 1

Composite Pu <sub>0.5</sub> Am <sub>0.5</sub> O <sub>2-x</sub> -MgO	(Pu <sub>0.5</sub> Am <sub>0.5</sub> )O <sub>2-x</sub> vol%	Theoretical density	Sintered density	% TD
PA20	20	5.11	4.92	96.4
PA30	30	5.85	5.55	94.8

Table 2

Composites	Phases	Formula	Lattice parameter a (Å)
PA20	bcc	Pu <sub>0.48</sub> <sup>4+</sup> Am <sub>0.02</sub> <sup>4+</sup> Am <sub>0.5</sub> <sup>3+</sup> O <sub>1.74</sub>	10.911
	fcc	Pu <sub>0.5</sub> <sup>4+</sup> Am <sub>0.26</sub> <sup>4+</sup> Am <sub>0.24</sub> <sup>3+</sup> O <sub>1.88</sub>	5.421
PA30	bcc	Pu <sub>0.32</sub> <sup>4+</sup> Pu <sub>0.18</sub> <sup>3+</sup> Am <sub>0.5</sub> <sup>3+</sup> O <sub>1.66</sub>	10.960
	fcc	Pu <sub>0.5</sub> <sup>4+</sup> Am <sub>0.36</sub> <sup>4+</sup> Am <sub>0.14</sub> <sup>3+</sup> O <sub>1.93</sub>	5.408

Table 3

**Figures:**

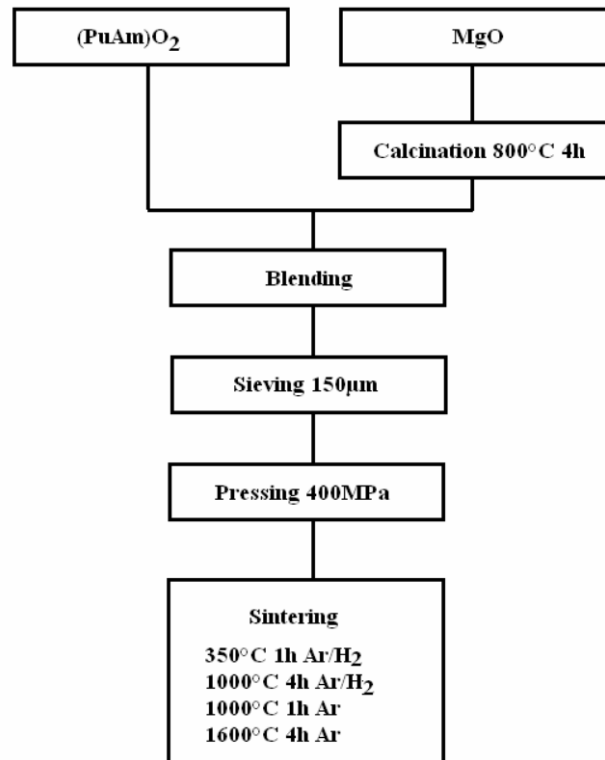


Figure 1

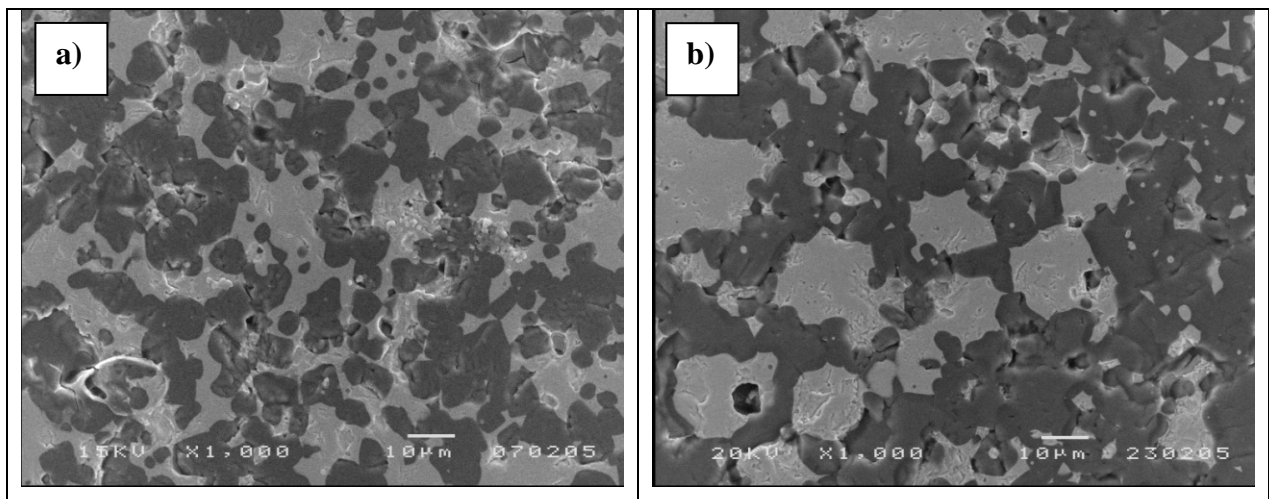


Figure 2 a -b

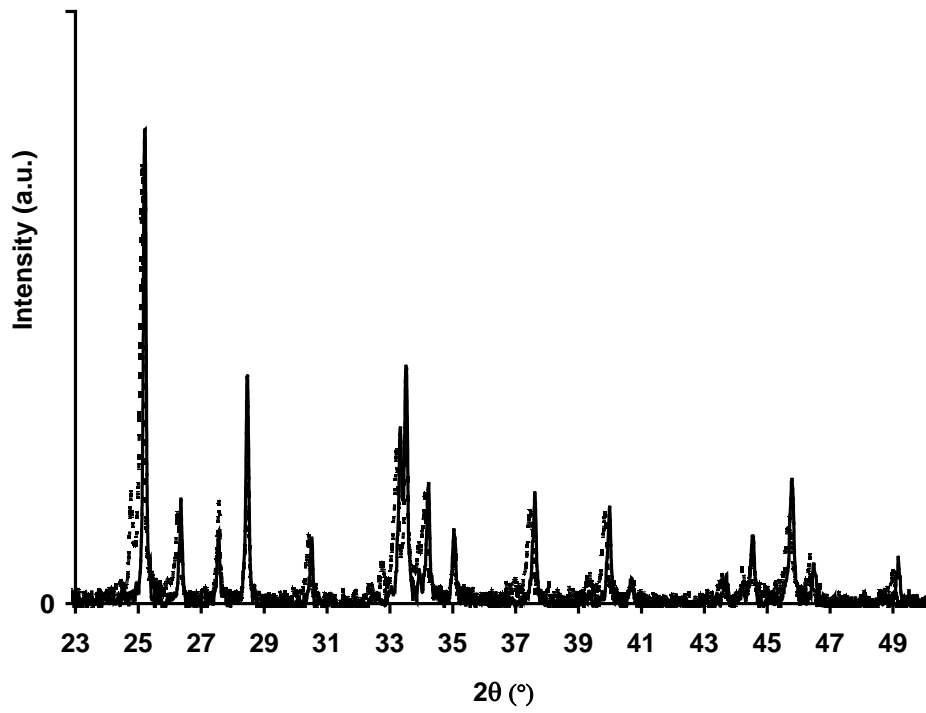


Figure 3

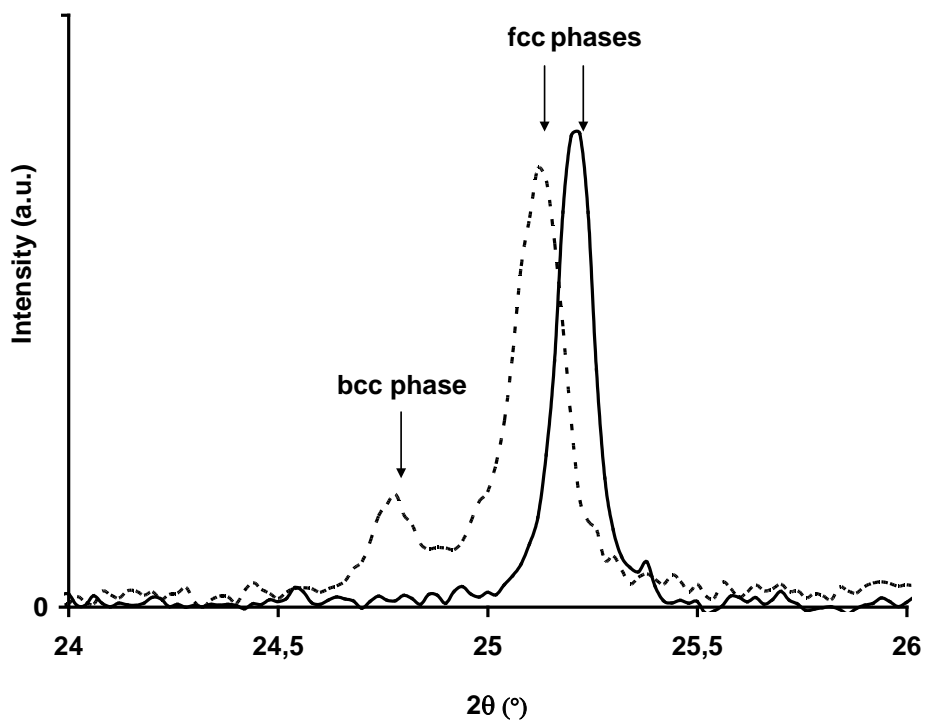


Figure 4

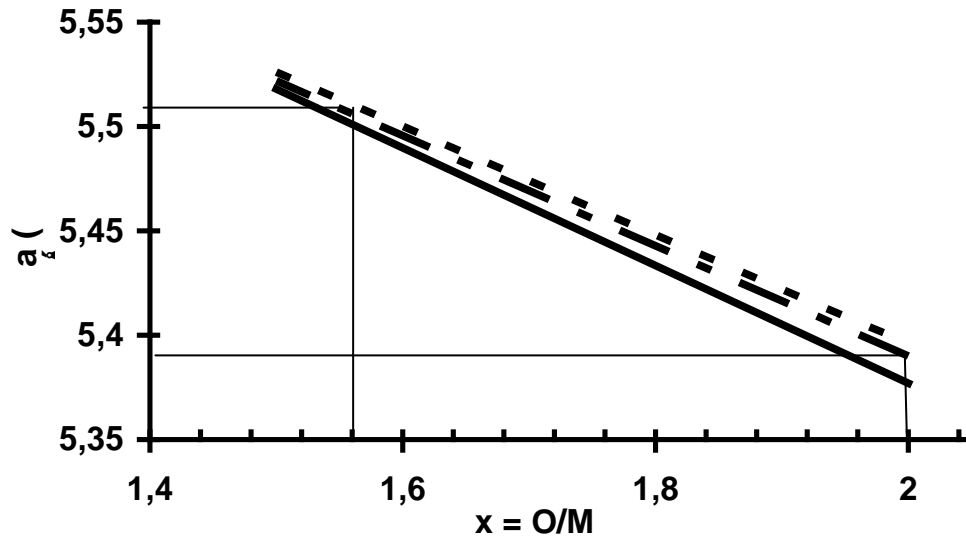


Figure 5

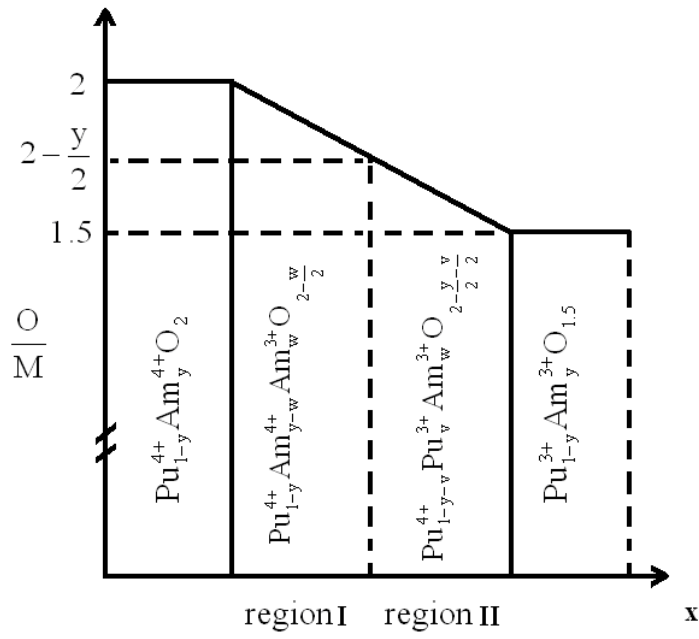


Figure 6

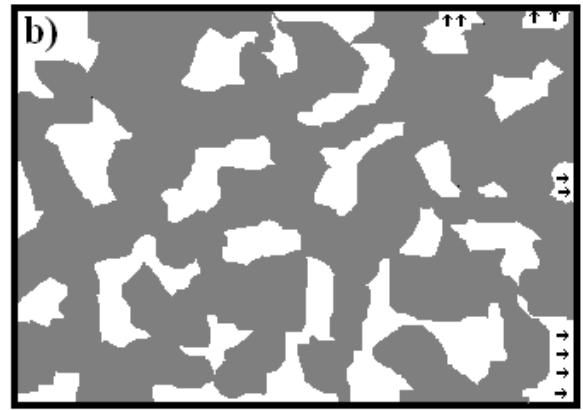
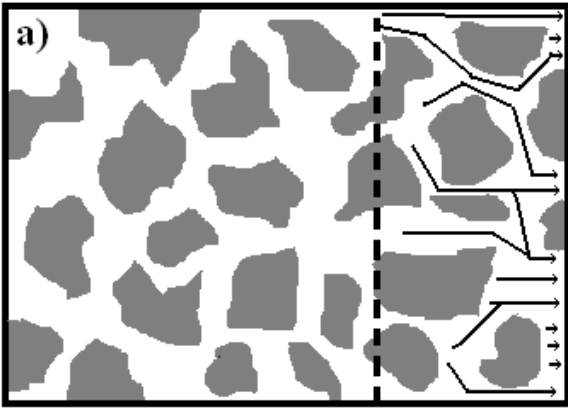


Figure 7 a-b

## References

---

- [1] D. Warin, F. Sudreau, S. Pillon, N. Drin, L. Donnet, E. Brunon, The FUTURIX-Transmutation Experiment in PHENIX, ATALANTE 2004, Nimes, June 2004.
- [2] P. Jaecki, S. Pillon, D. Warin, S.L. Hayes, J.R. Kennedy, K. Pasamehmetoglu, S.L. Voit, D. Haas, A. Fernandez, Y. Arai, Update on the FUTURIX-FTA Experiment in Phénix, Global 2005, Tsukuba, 2005.
- [3] G.A. Burney, Precipitation and coprecipitation of the transuranium elements from aqueous solution, Transurane D1, Gmelin Handbuch, 1975.
- [4] N. Cocuau, E. Picard, R.J.M. Konings, A. Conti, Hj. Matke, Inert matrices, uranium-free plutonium fuels and Americium targets. Synthesis of CAPRA, SPIN and EFTTRA studies, Global 97, Yokohama 1997.
- [5] Y. Croixmarie, E. Abonneau, A. Fernández, R. J. M. Konings, F. Desmoulière, L. Donnet, Fabrication of transmutation fuels and targets: the ECRIX and CAMIX-COCHIX experience, J. Nuc. Mat. Volume 320, Issues 1-2, (2003), 11-17.
- [6] A. Fernandez, R.J.M. Konings, J. Somers, Design and fabrication of specific ceramic-metallic fuels and targets, J. Nuc. Mat. 319, (2003), 44-50.
- [7] S. Casalta, Hj. Matzke, C. Prunier, Proceedings of the International Conference GLOBAL95, Versailles, 1995.
- [8] Masahiko Osaka, Ken Kurosaki, Shinsuke Yamanaka, Oxygen potential of  $(\text{Pu}_{0.91}\text{Am}_{0.09})\text{O}_{2-x}$ , J. Nuc. Mat. 357, (2006), 69-76.
- [9] H. Yoshimochi, M. Nemoto, S. Koyama, T. Namekawa, Fabrication technology for MOX fuel containing  $\text{AmO}_2$  by an In-cell remote process, J. Nucl. Sci. Technol. 41 (2004) 850.
- [10] L. Donnet, F. Jorion, N. Drin, S. L. Hayes, J. R. Kennedy, K. Pasamehmetoglu, S. L. Voit, D. Haas, A. Fernandez, The FUTURIX-FTA Experiment in PHENIX: Status of fuel fabrication, Proceedings of GLOBAL 2005, Tsukuba, 2005.
- [11] T. D. Chikalla, L. Eyring, Phase relationships in the americium-oxygen system, J. Inorg. Nucl. Chem Vol. 30, (1968), 133-145.
- [12] D.H. Templeton, C.H. Dauben, Lattice Parameters of Some Rare Earth Compounds and a Set of Crystal Radii, J. Amer. Chem. Soc., 75, 1953, 6069.
- [13] The Transuranium Elements Pt. II. New York, 1443, 1949.
- [14] S. Miwa, M. Osaka, H. Yoshimochi, K. Tanaka, K. Kurosaki, M.i Uno, S. Yamanaka, Phase behavior of  $\text{PuO}_{2-x}$  with addition of 9% Am, Jour. All. Comp. (available online 20 november 2006).

---

[15] C.Y. Tsai , C.-C Lin, A. Zangvil, A.-K Li, Effect of zirconia content on the oxidation behavior of silicon carbide/zirconia/mullite composites, J. Am. Ceram. Soc. vol. 81, [9], 1998, 2413-2420.

[16] Cheng-Yuan Tsai, Chien-Cheng Lin Dependence of Oxidation Modes on Zirconia Content in Silicon Carbide/Zirconia/Mullite Composites, J. Am. Ceram. Soc., Vol. 81, [12] 1998, 3150-3156.

[17] D.S. Mc Lachlan, M. Blaskiewicz, R. E. Newnham, Electrical resistivity of composites, J. Am. Ceram. Soc., 73 [8], 1990, 2187-2203.